GEOPHYSICAL RESEARCH LETTERS, VOL. 35, L12603, doi:10.1029/2008GL033957, 2008

Oceanic mesoscale eddies as revealed by Lagrangian coherent structures

F. J. Beron-Vera,[1] M. J. Olascoaga,[1] and G. J. Goni[2]

Received 13 March 2008; revised 17 April 2008; accepted 2 May 2008; published 19 June 2008.

[1] We demonstrate the feasibility of using dynamical systems tools to unambiguously identify mesoscale oceanic eddies from surface ocean currents derived using climatological hydrography and altimetry. Specifically, our analysis is based on extracting Lagrangian coherent structures (LCSs) from finite-time Lyapunov exponent (FTLE) fields. The FTLE fields reveal with unprecedented detail an intricate tangle of LCSs, which are hidden in ocean surface topography maps but sometimes are apparent in ocean color images. These LCSs delineate fluid domains with very different advective properties, and thus their detection provides an objective (i.e., frame-independent) means of identifying eddy boundaries. The importance of considering LCSs in quantifying transport by eddies is highlighted. Such a quantification does not rely on the common assumption—which is shown to be generally not valid—that transport is largely effected by the trapping and subsequent translation of water slugs inside eddies defined as the regions enclosed by sea height (streamfunction) contours within which rotation dominates over strain. LCSs are calculated for the whole globe and compared with satellite-tracked drogue drifter trajectories within a selected region of the South Atlantic. **Citation:** Beron-Vera, F. J., M. J. Olascoaga, and G. J. Goni (2008), Oceanic mesoscale eddies as revealed by Lagrangian coherent structures, *Geophys. Res. Lett.*, *35*, L12603, doi:10.1029/2008GL033957.

1. Introduction

[2] Oceanic mesoscale eddies are commonly identified as regions enclosed by sea height (streamfunction) contours within which water slugs of unique characteristics are trapped and subsequently translated [e.g., *Witter and Gordon*, 1999; *Goni and Johns*, 2001]. Using Lagrangian coherent structures (LCSs), a recently developed dynamical systems concept, in this work: (i) we demonstrate the feasibility of unambiguously identifying eddies; and (ii) we provide evidence that the above common picture is generally not valid. Our analysis is based on ocean surface velocities inferred using climatological hydrographic observations and altimetric sea height measurements. Unlike prior work [e.g., *d'Ovidio et al.*, 2004; *Shadden et al.*, 2005], LCSs are computed for the whole globe and compared with satellite-tracked drogue drifter trajectories in a selected region of the South Atlantic. Also, our results emphasize the importance of considering LCSs in producing quantitative estimates of transport by eddies.

2. Methods

[3] A LCS can be regarded as a material line such that fluid particles straddling it either diverge or converge in forward time. In the first case the LCS is called repelling, while in the second case is called attracting [*Haller and Yuan*, 2000]. LCSs thus delineate the boundary between fluid domains with quite distinct advection characteristics, which cannot be revealed visually by inspecting velocity field snapshots. This property of LCSs has allowed for an objective (i.e, frame-independent) eddy boundary definition [*Haller*, 2001; *Green et al.*, 2007], and is exploited here to unambiguously reveal mesoscale oceanic eddies with a sea surface signature. It must be noted, however, that attracting and repelling LCSs in unsteady flows do not coincide as in steady flows, but typically transversely intersect each other many times. The intersection of attracting and repelling LCSs define "lobes" which enclose fluid that must remain so over time due to the material nature of the LCSs. Consequently, the exchange of eddy and ambient fluid (including neighboring vortices fluid) in unsteady flows is not prevented by the LCSs, but rather effectively accomplished by their deformation over time [*Shadden et al.*, 2006; *Franco et al.*, 2007]. The range of the fluid exchange depends on the amount of deformation experienced by the LCSs.

[4] Computation of finite-time Lyapunov exponents (FTLEs) constitutes a practical and robust means of identifying LCSs [*Haller*, 2001; *Shadden et al.*, 2005; *Mathur et al.*, 2007]. The FTLE is a scalar measure of the finite-time separation rate of neighboring fluid particles, which may be conveniently defined as

$$\sigma^{\tau}_{t_0}(\lambda_0,\vartheta_0) := |\tau|^{-1} \ln ||\Delta^{\tau}_{t_0}(\lambda_0,\vartheta_0)||, \tag{1}$$

where $\|\ \|$ denotes largest singular value and

$$\Delta^{\tau}_{t_0}(\lambda_0,\vartheta_0) := \begin{pmatrix} \partial_{\lambda_0}\lambda(t_0+\tau;\lambda_0,\vartheta_0,t_0)\,\partial_{\vartheta_0}\lambda(t_0+\tau;\lambda_0,\vartheta_0,t_0) \\ \\ \partial_{\lambda_0}\vartheta(t_0+\tau;\lambda_0,\vartheta_0,t_0)\,\partial_{\vartheta_0}\vartheta(t_0+\tau;\lambda_0,\vartheta_0,t_0) \end{pmatrix}, \tag{2}$$

which measures the change in the fluid particle longitude–latitude position on the sea surface at $t = t_0 + \tau$, $(\lambda(t_0+\tau;\lambda_0,\vartheta_0,t_0), \vartheta(t_0+\tau;\lambda_0,\vartheta_0,t_0))$, induced by an infinitesimal change in its position at time $t = t_0$, (λ_0, ϑ_0). The position at

[1] Rosenstiel School of Marine and Atmospheric Science, University of Miami, Miami, Florida, USA.
[2] Atlantic Oceanographic and Meteorological Laboratory, National Oceanic and Atmospheric Administration, Miami, Florida, USA.

0094-8276/08/2008GL033957$05.00

any time $t \neq t_0$ is obtained by integrating the trajectory equations

$$\dot{\lambda} = a^{-1}\sec\vartheta\, u(\lambda,\vartheta,t), \qquad \dot{\vartheta} = a^{-1}v(\lambda,\vartheta,t), \tag{3}$$

where the overdot stands for time differentiation; a is the earth's mean radius; and u (v) is the northward (eastward) sea surface velocity component. Regions of maximum separation rates produce local maximizing curves or "ridges" in the FTLE field, which approximate LCSs. When the FTLE is computed by integrating particle trajectories forward (backward) in time, $\tau > 0$ ($\tau < 0$), ridges in the FTLE field corresponds to repelling (attracting) LCSs.

[5] We have chosen to consider a sea surface flow described by

$$u = -g(fa)^{-1}\partial_\vartheta\eta, \qquad v = g(fa\cos\vartheta)^{-1}\partial_\lambda\eta, \tag{4}$$

where g is gravity; $f := 2\Omega\sin\vartheta$ is the Coriolis parameter, with Ω the earth's angular speed; and η is the sea height. The background (steady) η component is taken to be the mean dynamic topography relative to 1000 m, which was computed using climatological observations of temperature and salinity [*Conkright et al.*, 2002]. The perturbation (transient) η component is given by altimetric sea height anomaly measurements provided weekly on a 0.25° latitude $\times$ 0.25° longitude grid and referenced to a 7-year (1993–1999) mean, which were obtained from the combined processing of Jason-1, TOPEX/Poseidon, ENVISAT, GFO, ERS-1 and -2, and GEOSAT altimeters [*Le Traon et al.*, 1998; *Ducet et al.*, 2000].

[6] FTLE fields were produced by direct finite differentiation of trajectories on regular grids with a resolution two (Figure 1) and six (Figures 2–4) times finer than the velocity field grid, which allowed us to reveal LCSs with great detail. The trajectory integrations were performed using a fourth-order Runge–Kutta method with a daily timestep; the required velocity interpolations were done using a linear scheme. The choice $|\tau|$ = 60 d was found enough to fairly resolve mesoscale structures ($|\tau|$ can be varied depending on the amount of detail desired without affecting the position of the FTLE ridge indicating the LCS [*Green et al.*, 2007]). The LCS computations were tested using satellite-tracked drogue drifter data obtained from the NOAA/AOML Drifter Data Assembly Center, which consisted of daily drifter positions subsampled from the hourly raw drifter positions, previously lowpass-filtered with a 5-day cutoff.

3. Results

[7] Figure 1 shows a typical global snapshot of backward-time FTLE field. Excluded only are world ocean areas shallower than 1000 m and the ±5° latitudinal band around the equator, where (4) breaks down. The regions of most intense red tones roughly indicate FTLE field ridges. These regions are seen to form seemingly smooth, albeit structured, curves that constitute the desired LCSs. A close inspection of this FTLE field reveals with unprecedented detail a very rich variety of LCSs, including spiral- and mushroom-like LCSs, which may sometimes be observed in ocean color images. The spiral-like LCSs correspond to distorted monopolar (cyclonic or anticyclonic) eddies. The mushroom-like LCSs may be identified with distorted dipolar (cyclonic and anticyclonic) eddies. Except in the tropics, the lengthscale of these LCSs is a few times larger than the first baroclinic deformation radius. This is consistent with the idea [*Stammer*, 1997; *Scott and Wang*, 2005] that baroclinic instability is an important source of eddy kinetic energy, whose spatial distribution is well-correlated with that of FTLEs. The revealed LCSs typically persist during several months while undergo vigorous deformation.

[8] Figure 2a shows a blow-up of the region indicated in Figure 1. The FTLE field shown in Figure 2a reveals with greater detail the LCS types described above. Note, for instance, the prominent mushroom-like LCS near the lower-right corner of the dashed box. Figure 2b shows the sea surface topography map corresponding to the date on which the FTLEs were computed. Clearly, the topology of the LCSs described above cannot be inferred visually from inspection of this map: η contours bear no resemblance with the LCSs. Figure 2c depicts on the same date the Okubo–Weiss (OW) parameter [*Okubo*, 1970; *Weiss*, 1991]

$$Q := \left(\omega + 2a^{-1}\tan\vartheta\, u\right)^2 - n^2 - s^2 \tag{5}$$

where $\omega := a^{-1}(\tan\vartheta\ \partial_\lambda v - \partial_\vartheta u)$ (the relative vorticity is $\omega + a^{-1}\tan\vartheta\, u$); $n := a^{-1}(\sec\vartheta\ \partial_\lambda u - \partial_\vartheta v - \tan\vartheta\ v)$ is the normal component of strain; and $s := a^{-1}(\sec\vartheta\ \partial_\lambda u + \partial_\vartheta u)$ is the shear component of strain. According to the OW criterion, an Eulerian coherent structure is defined as a region where rotation dominates over strain, i.e., $Q > 0$. Superimposed on the Q field are isolines of Q corresponding to two-standard deviations of Q in the whole domain; similar thresholds have been previously adopted [e.g., *Isern-Fontanet et al.*, 2003; *Morrow et al.*, 2004; *Chelton et al.*, 2007]. Comparison of Figures 2a and 2c shows that the OW criterion does not reveal all the structures uncovered using the FTLE method, even if Q is plotted assuming a very small threshold.

[9] Figure 3 shows a roughly three-month-long sequence of snapshots of backward-time FTLE fields for initial fluid particle positions falling within the dashed box in Figure 2a. In this region the FTLE method identifies a great deal of LCSs while the OW criterion indicates the presence of almost no structure. Note that each identified LCS can be smoothly tracked over time in the sequence of FTLE field snapshots shown. Overlaid on each FTLE field depicted in Figure 3 is the instantaneous position of a satellite-tracked drogue drifter. The trajectory of this drifter is shown in Figure 3g. A blue dot in Figure 3g corresponds to the drifter position on the date in which it is superimposed on the corresponding FTLE field. Note the deformation process suffered by the mushroom-like LCS on the left of the big mushroom-like LCS seen on 20 April 2005. After being sucked into this LCS, the drifter closely follows this deformation process. The tendency of the drifter to closely follow the pathway determined by the LCSs revealed in the backward-time FTLE fields demonstrates that the estimated surface ocean LCSs in the region considered constitute to a very good approximation attracting material curves. Inspection of other drifter trajectories were also found to exhibit similar tendency. (Animations revealing this tendency are

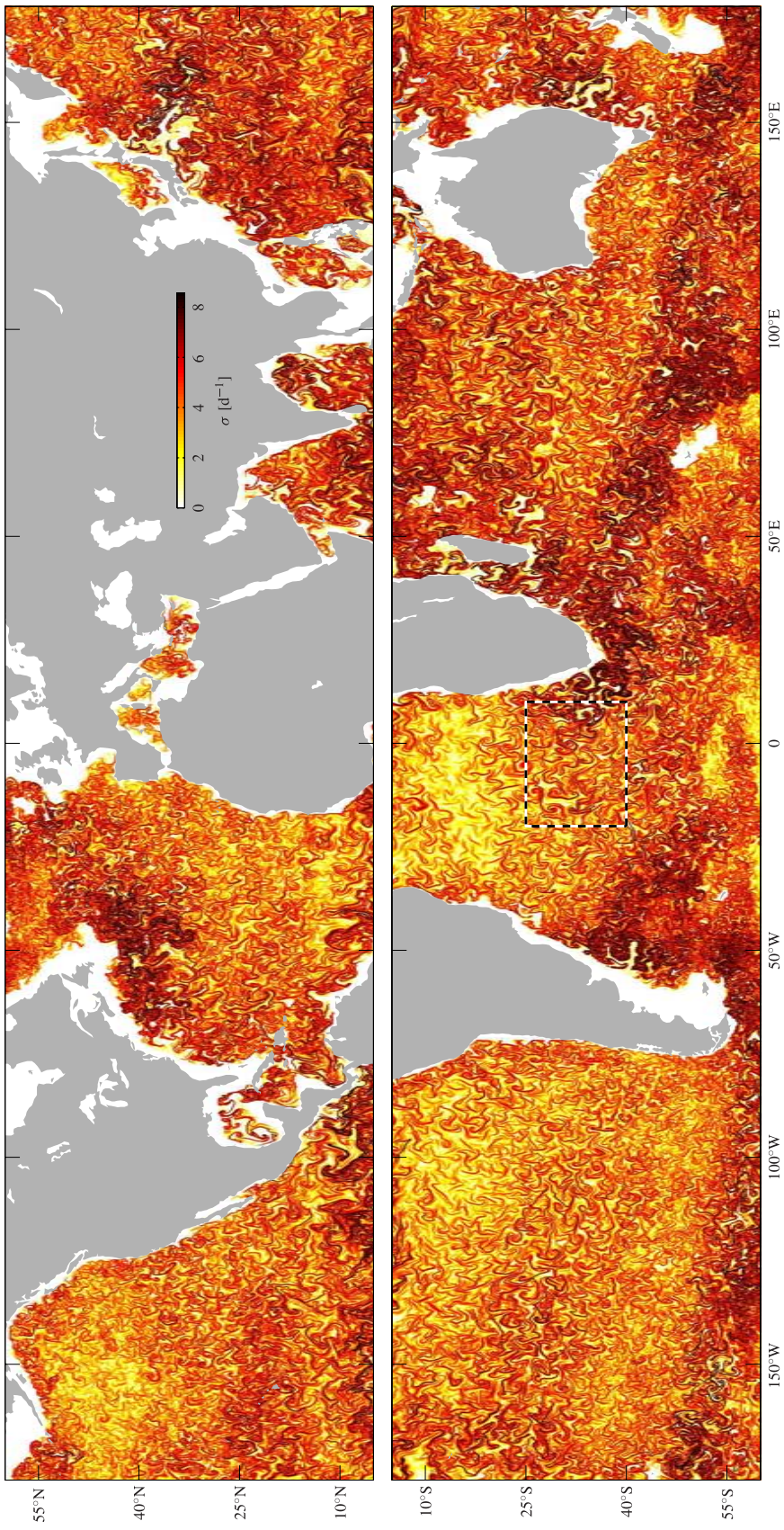

Figure 1. A global snapshot of backward-time FTLE field (1) on 20 April 2005 computed using sea surface velocities inferred from climatological hydrography and altimetry. LCSs roughly correspond to regions of most intense red tones.

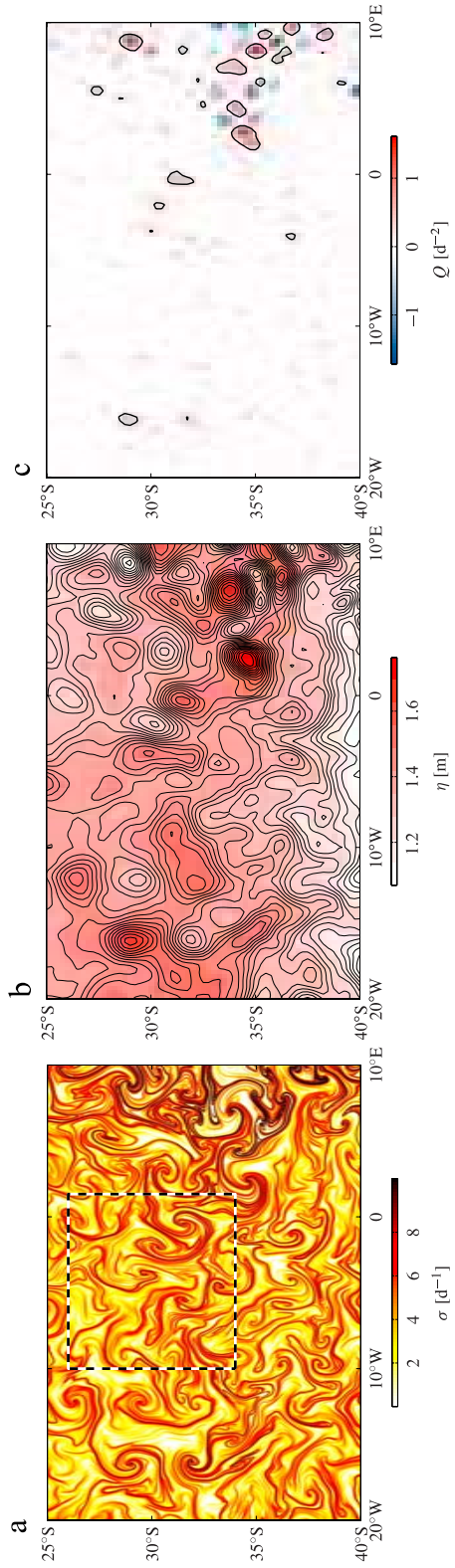

Figure 2. (a) Blow-up of the region indicated in Figure 1, (b) corresponding sea surface topography map, and (c) OW parameter. Indicated in Figure 2a is the region where the FTLEs shown in Figure 3 were computed.

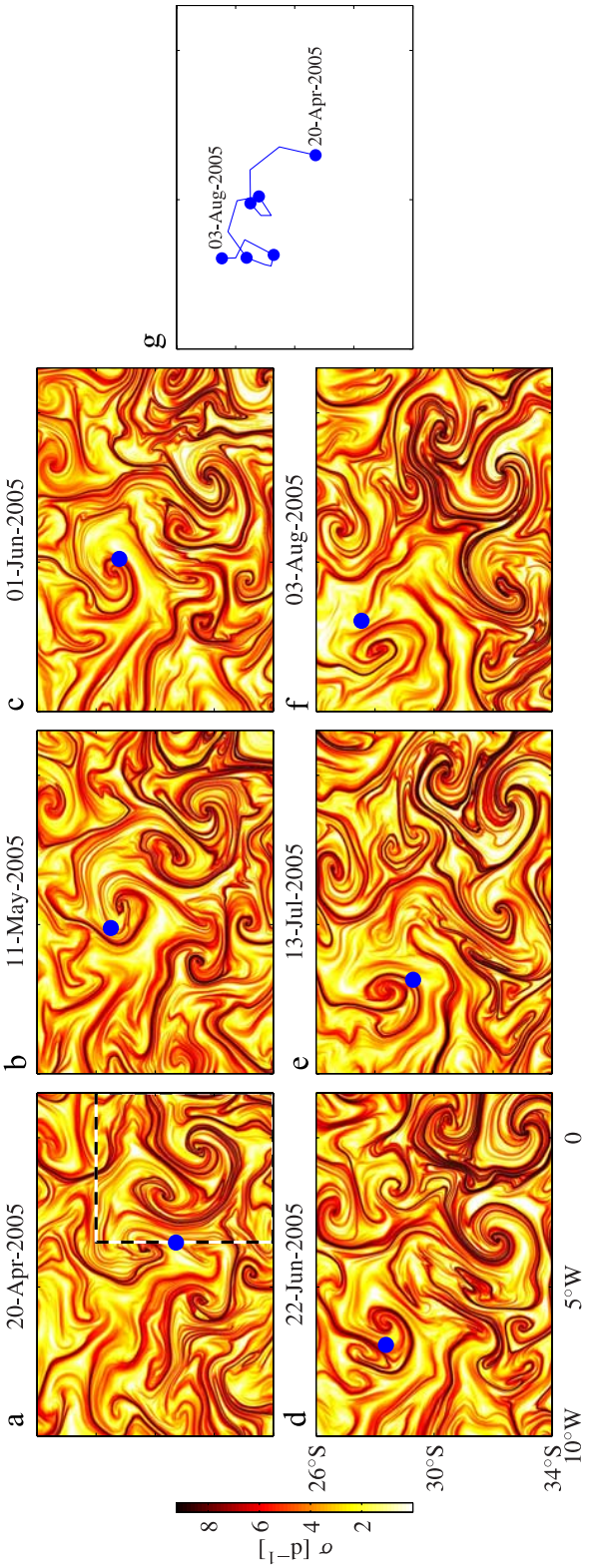

Figure 3. Sequence of FTLE field snapshots for initial fluid particle positions within the dashed box in Figure 2a. Overlaid on each FTLE field is the instantaneous position of a satellite-tracked drogue drifter (blue dot) whose trajectory is depicted in Figure 3g.

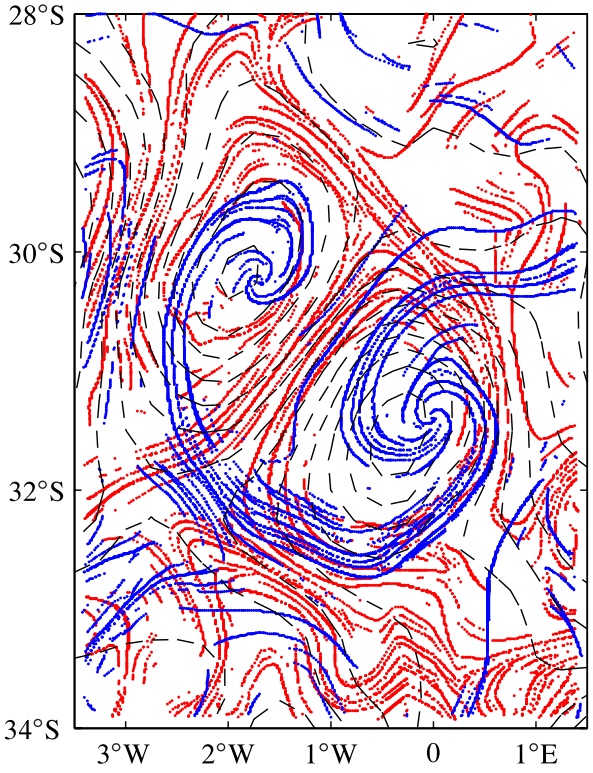

Figure 4. Attracting (red) and repelling (blue) LCSs extracted from FTLE fields computed backward and forward in time, respectively, for initial fluid particle positions on 20 April 2005 within the dashed box in Figure 3a. Dashed lines indicate sea surface topography contours.

available at ftp://ftp.rsmas.miami.edu/users/fberon/lcsvortex.) Given the spatiotemporal coarseness of the velocity data, this remarkable result suggests that passive tracer evolution over weeks to several months is governed to a good extent by spectrally nonlocal dynamics in the region considered. Non-Guassian probability distribution of FTLEs and steep kinetic energy spectrum (not shown) further support this notion.

[10] Figure 4 finally shows both attracting and repelling LCSs on 20 April 2005 within the dashed box in Figure 3a. These LCSs were computed as in *Mathur et al.* [2007] by noting that, for fixed t_0 and large enough τ, LCSs constitute attracting sets of the gradient system

$$\lambda_0' = a^{-1}\partial_{\lambda_0}\sigma^{\tau}_{t_0}, \qquad \vartheta_0' = a^{-1}\sec\vartheta_0\,\partial_{\vartheta_0}\sigma^{\tau}_{t_0}, \tag{6}$$

where the prime indicates differentiation with respect to the arclength along FTLE gradient lines. This follows immediately from the fact that LCSs are FTLE field ridges. Figure 4 shows a highly intricate LCS tangle wherein attracting LCSs (red curves) and repelling LCSs (blue curves) transversely intersect one another many times, which constitutes a template for eddy–ambient water mixing. Note also that these LCSs intersect η contours (dashed lines in Figure 4) thereby allowing for fluid entrainment and detrainment through these contours as the LCSs wrap around them over time. This shows that identification of the closed η contours depicted in this figure with two isolated eddies which trap and subsequently translate water slugs that retain their characteristics is not valid. Rather, the LCSs reveal a distorted dipolar eddy which vigorously exchanges water with the surrounding water along its path (Figure 3). An appropriate exchange boundary is defined by the LCSs up to their intersection points, which may in principle be systematically identified (*Franco et al.*, 2007). The mechanism for these exchanges is the deformation of the attracting and repelling LCSs over time, which cannot be inferred visually from the inspection of the corresponding sea surface topography maps or the OW parameter distributions.

4. Discussion

[11] Transport is an inherently Lagrangian notion. Consequently, the correct estimation of transport by mesoscale oceanic eddies must account for the fluid particle motion information carried by LCSs, which we have demonstrated that can be feasibly extracted from surface ocean currents derived using climatological hydrography and altimetry. Specific questions that may be studied by revealing surface ocean LCSs include the following. What is the extent of the eddy–ambient water exchange? What is the fraction of water transported by eddies preserving its characteristics? What is the distance that water fraction travels across the ocean? Addressing these questions is critical to correctly assess the role of eddies as transport agents. Given the intricate nature of the surface ocean LCSs, however, their systematic use in addressing the above questions represents a challenge.

[12] **Acknowledgments.** We thank M. Brown, H. Koçak, I. Rypina, and I. Udovydchenkov for the benefit of helpful discussions on dynamical systems. The altimeter products were produced by SSALTO/DUACS and distributed by AVISO, with support from CNES. FJBV and MJO were supported by NSF grant CMG0417425. GJG was supported by NOAA/CPO.

References

Chelton, D. B., M. G. Schlax, R. M. Samelson, and R. A. de Szoeke (2007), Global observations of large oceanic eddies, *Geophys. Res. Lett.*, *34*, L15606, doi:10.1029/2007GL030812.

Conkright, M. E., et al. (2002), World Ocean Database 2001, Volume 1: Introduction, 152 pp., NOAA Atlas NESDIS 42, U.S. Government Printing Office, Washington, D.C.

d'Ovidio, F., V. Fernández, E. Hernández-Gracía, and C. López (2004), Mixing structures in the Mediterranean Sea from finite-size Lyapunov exponents, *Geophys. Res. Lett.*, *31*, L17203, doi:10.1029/2004GL020328.

Ducet, N., P.-Y. Le Traon, and G. Reverdin (2000), Global high resolution mapping of ocean circulation from TOPEX/Poseidon and ERS-1 and -2, *J. Geophys. Res.*, *105*, 19,477–19,498.

Franco, E., D. N. Pekarek, J. Peng, and J. O. Dabiri (2007), Geometry of unsteady fluid transport during fluid-structure interactions, *J. Fluid Mech.*, *589*, 125–145.

Goni, G., and W. Johns (2001), Census of warm rings and eddies in the North Brazil Current retroflection region from 1992 through 1998 using TOPEX/Poseidon altimeter data, *Geophys. Res. Lett.*, *28*, 1–4.

Green, M. A., C. W. Rowley, and G. Haller (2007), Detection of Lagrangian coherent structures in three-dimensional turbulence, *J. Fluid Mech.*, *572*, 111–120, doi:10.1017/S0022112006003648.

Haller, G. (2001), Lagrangian structures and the rate of starin in a partition of two-dimensional turbulence, *Phys. Fluids*, *13*, 3365–3385.

Haller, G., and G. Yuan (2000), Lagrangian coherent structures and mixing in two-dimensional turbulence, *Physica D*, *147*, 352–370.

Isern-Fontanet, J., E. García-Ladona, and J. Font (2003), Identification of marine eddies from altimetric maps, *J. Atmos. Oceanic Technol.*, *20*, 772–778.

Le Traon, P.-Y., F. Nadal, and N. Ducet (1998), An improved mapping method of multisatellite altimeter data, *J. Atmos. Oceanic Technol.*, *15*, 522–534.

Mathur, M., G. Haller, T. Peacock, J. E. Ruppert-Felsot, and H. L. Swinney (2007), Uncovering the Lagrangian skeleton of turbulence, *Phys. Rev. Lett.*, *98*, 144,502, doi:10.1103/PhysRevLett.98.144502.

Morrow, R., F. Birol, and D. Griffin (2004), Divergent pathways of cyclonic and anti-cyclonic ocean eddies, *Geophys. Res. Lett.*, *31*, L24311, doi:10.1029/2004GL020974.

Okubo, A. (1970), Horizontal dispersion of flotable particles in the vicinity of velocity singularity such as convergences, *Deep-Sea Res. Oceanogr. Abstr.*, *12*, 445–454.

Scott, R. B., and F. Wang (2005), Direct evidence of an oceanic inverse kinetic energy cascade from satellite altimetry, *J. Phys. Oceanogr.*, *35*, 1650–1666.

Shadden, S. C., F. Lekien, and J. E. Marsden (2005), Definition and properties of Lagrangian coherent structures from finite-time Lyapunov exponents in two-dimensional aperiodic flows, *Physica D*, *212*, 271–304.

Shadden, S. C., J. O. Dabiri, and J. E. Marsden (2006), Lagrangian analysis of fluid transport in empirical vortex ring flows, *Phys. Fluids*, *18*, 47,105.

Stammer, D. (1997), Global characteristics of ocean variability estimated from regional TOPEX/POSIDON altimeter measurements, *J. Phys. Oceanogr.*, *27*, 1743–1769.

Weiss, J. (1991), The dynamics of enstrophy transfer in two-dimensional hydrodynamics, *Physica D*, *48*, 273–294, doi:10.1016/0167-2789(91)90088-Q.

Witter, D. L., and A. L. Gordon (1999), Interannual variability of the South Atlantic circulation from 4 years of TOPEX/POSEIDON satellite altimeter observations, *J. Geophys. Res.*, *10*, 20,927–20,948.

F. J. Beron-Vera and M. J. Olascoaga, UM/RSMAS/AMP, 4600 Rickenbacker Causeway, Miami, FL 33149, USA. (fberon@rsmas.miami.edu)

G. J. Goni, NOAA/AOML/PhOD, 4301 Rickenbacker Cswy., Miami, FL 33139, USA.